Molecular Crystals and Liquid Crystals
Publication details, including instructions for authors and subscription information:
http://www.tandfonline.com/loi/gmcl18

Prominent Effect of Electric Field to Nonlinear Wave Mixing Process in Liquid Crystals

Shu-Hsia Chen [a] & Chen-Lung Kuo [a]
[a] Institute of Electro-Optical Engineering, National Chiao Tung University, Hsinchu, Taiwan, 30050, R. O. C.
Version of record first published: 24 Sep 2006.

To cite this article: Shu-Hsia Chen & Chen-Lung Kuo (1991): Prominent Effect of Electric Field to Nonlinear Wave Mixing Process in Liquid Crystals, Molecular Crystals and Liquid Crystals, 207:1, 131-149

To link to this article: http://dx.doi.org/10.1080/10587259108032094

Mol. Cryst. Liq. Cryst., 1991, Vol. 207, pp. 131–149
Reprints available directly from the publisher
Photocopying permitted by license only

Printed in the United States of America

PROMINENT EFFECT OF ELECTRIC FIELD TO NONLINEAR WAVE MIXING PROCESS IN LIQUID CRYSTALS

SHU-HSIA CHEN AND CHEN-LUNG KUO
Institute of Electro-Optical Engineering, National Chiao Tung University, Hsinchu, Taiwan 30050, R. O. C.

Abstract The nonlinear wave mixing process in liquid crystals due to field-induced molecular reorientation is studied. Prominent effect of electric field to this nonlinear optical process is illustrated by optimizing the diffraction efficiency of degenerate four-wave mixing process in nematics. The nonlinear refrative-index change is shown not only dependent on the electric bias and material parameters but also on the experimental geometry, such as the sample thickness and the grating period. The numerical and experimental results exhibiting the characteristic behaviors of this process are summarized. The unique effect of electric bias is emphasized by comparing the diffraction efficiency with that of the phase grating induced by oblique incident laser beams.

INTRODUCTION

It is well know that liquid crystals are extraordinary nonlinear optical media. Even with CW laser, the nonlinear optical effects, such as self-focusing, self phase modulation, optical bistability and degenerate wave-mixing are readily observable in liquid crystals. Their extremely high optical nonlinearities make them potentially useful for optoelectronic devices. In the meantime, the electric field plays an

important roles in nonlinear optical phenomena in liquid crystals. For example, a quasi-static electric field can enhance laser-induced diffraction rings from a nematic liquid-crystal film[1] . The optical bistability can be induced in nematic liquid crystals by applying an electric field[2]. In this paper we summarize the results of our works on electric-field biased degenerate four-wave mixing (DFWM) process in nematic liquid crystals.

In nematic liquid crystals (NLC), the molecular reorientation and its associated nonlinear refractive-index change Δn_{NL} are subjected to the interaction between the dielectric torques exerted by the resultant fields and the elastic restoring torques of NLC.

The nonlinear coupling coefficient in the coupled-wave equations, which are usually used to describe the nonlinear wave-mixing process[3], is not a constant for this system. It depends not only on material parameters but also on the experimental geometry, i.e. the distorted structure in NLC. Consequently, in order to know the detail of the nonlinear coefficient, the local molecular reorientation must be found by continuum theory. And DFWM can be described by diffraction from an induce phase grating for a sufficiently thin film.

In earlier studies[4], one-elastic-constant approximation was made in deriving the theoretical model and the twist deformation in the system was disregarded. With the presence of magnetic field, it was reported[5] that the diffraction efficiency is a monotonically decreasing function of the biased field and the highest efficiency is always obtained at the freedericksz threshold value.

In 1989, we presented a modified theoretical model by considering the twist effects in a low-frequency electric-field-biased NLC sample[6]. We reported the first successful explanation of the diffraction peak shift and illustrated the dramatic suppression of the diffraction efficiency. The twist deformation is the crucial factor accounted for these phenomena. Large peak shift and suppression of diffraction efficiency were obtained in the experiment and calculation. In a latter study, it was found that peaks of the same efficiency can be observed at two distinct voltages if the phase amplitude of the induced grating is large enough[7]. By removing the assumption of one-elastic-constant approximation in the theoretical model, it was concluded that the difference of the bend and splay elastic constants for the NLC medium could influence the optimal bias drastically, in addition to the twist deformation[8]. It was shown that the optimal amplitude of the induced phase grating

is a monotonically increasing function of the grating period, the optical intensity, and the ratio of the bend elastic constant to that of twist. However, the dependence of the phase amplitude on the sample thickness is quite unique[9]. There always exists an optimal thickness for the peak phase amplitude.

In the following sections, a general description of the theory is presented at first. An expression of non-constant Kerr coefficient is derived. The numerical and experimental results which support the theoretical model for forward-wave interaction DFWM are then summarized. The influence of the biased electric field on the backward interaction is illustrated both numerically and experimentally by the behavior of its diffraction efficiency. Numerical results of optimal reorientation-angle modulation and phase amplitude for oblique incident geometry are obtained by utilizing the model[10] of Fuh *etal* 's. These results are compared with that of ours for the normal incident geometry with biased electric field.

THEORY

Consider a homeotropically aligned nematic liquid-crystal cell of thickness d with nearly normally incident laser beams as shown in Figure 1. The nematic substance is

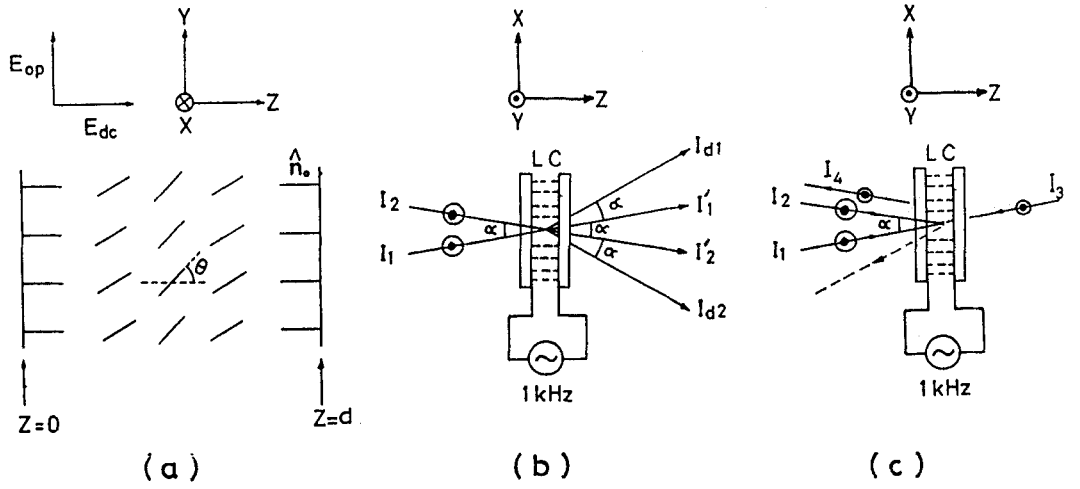

FIGURE 1 Schematic diagram of DFWM in an electric-field-biased nematic film.. (a) Structure of molecular reorientation. (b) Forward-wave interaction geometry. (c) Backward interaction geometry.

assumed to have positive optical and negative dielectric anisotropies, namely, $n_e > n_o$ and $\epsilon_{\parallel} < \epsilon_{\perp}$ where n and ϵ denote the refractive indices and dielectric constants, and the subscripts refer to the directions parallel and perpendicular to the director, respectively. For a sufficiently thin sample, degenerate four-wave mixing can be simply described by diffraction from an induced phase grating. The picture is that the interference of two linearly polarized laser beams with intensities I_1 and I_2, respectively, produces a sinusoidlly varying intensity pattern, $I=I_1 + I_2 + 2\sqrt{I_1 I_2}$ cos $(2\pi x/\Lambda)$, in the sample with a period Λ. The optical fields superpose to the applied electric field and create a periodically distorted molecular-reorientation structure, which then gives rise to an induced phase grating with the same period. This phase grating diffracts the original incident beams (forward interaction), or the reverse pumping beam (backward interaction), into both sides. Here we limit ourself in the case of lowest-order diffraction.

Instead of using one-elastic-constant approximation, a general form which includes splay, twist and bend terms is used for the free energy density $\mathcal{F}$ as following

$$\mathcal{F} = \frac{1}{2}[\, K_2(\frac{\partial\theta}{\partial x})^2 + K_3(1\text{-}K \sin^2\theta)(\frac{\partial\theta}{\partial z})^2] - \frac{D_z^2}{8\pi\epsilon_{\parallel}} \frac{1}{1\text{-}w \sin^2\theta} - \frac{I}{c} \frac{n_0}{\sqrt{1\text{-}u \sin^2\theta}} \qquad (1)$$

where $K \equiv 1\text{-}K_1 / K_3$, $u = 1\text{-}n_o^2 / n_e^2$, $w = 1\text{-} \epsilon_{\perp} / \epsilon_{\parallel}$; K_1, K_2, K_3 represent the splay, twist and bend elastic constants, respectively; D_z is the z component of the electric displacement; I is the optical intensity and c is the velocity of light in vacuum. We treat the forward interaction at first and use a trial solution for the reorientational angle of local average,

$$\theta(x,z) = [\theta_1 + \theta_2 \cos(2\pi x/\Lambda)] \sin(\pi z/d),$$

with the boundary condition: $\theta(z=o) = \theta(z=d) = 0$. Here θ_1 and θ_2 represent the transverse spatial average of orientational angle and the amplitude of the modulation orientational angle, respectively. The equilibrium values of the constants θ_1 and θ_2 can be calculated from the minimization of the total free energy, $F=\int \mathcal{F} dv$, by letting $\partial F/\partial\theta_1=0$ and $\partial F/\partial\theta_2=0$, we then have

$$\theta_1 - KG_1(\theta_1,\theta_2) - (V/V_{th})^2 G_2(\theta_1,\theta_2) - I_r G_3(\theta_1,\theta_2) + (I_t/I_{th}) G_4(\theta_1,\theta_2) = 0 \qquad (2)$$

and

$$\theta_2[1+ 2a - KG_5(\theta_1,\theta_2)] - 2I_r J_1(2\theta_1) - [(I_t/I_{th}) + (V/V_{th})^2] G_3(\theta_1,\theta_2) = 0 \qquad (3)$$

with the functions representing

$$\begin{aligned}
G_1(\theta_1,\theta_2) = {} & \theta_1 / 2 \\
& + J_0(2\theta_1)(\theta_1\theta_2^2 / 8 - \theta_1 / 2) \\
& + J_1(2\theta_1)(\theta_1^2 / 4 - \theta_1^2\theta_2^2 / 8 - 3\theta_2^4 / 32 + 5\theta_2^2 / 8) \\
& - J_2(2\theta_1)\, \theta_1 / 2 \\
& + J_3(2\theta_1)(\theta_1^2/4 - \theta_1^2\theta_2^2/16 - 3\theta_2^2/8 - 3\theta_2^4/64) \\
& - J_4(2\theta_1)\theta_1\theta_2^2/8 \\
& + J_5(2\theta_1)(3\theta_2^4/64 + \theta_1^2\theta_2^2/16) \\
G_2(\theta_1,\theta_2) = {} & J_3(2\theta_1)\theta_2^2/4 + J_1(2\theta_1)(2 - 3\theta_2^2/2)/2 \\
G_3(\theta_1,\theta_2) = {} & \theta_2[J_0(2\theta_1) - J_2(2\theta_1)] \\
G_4(\theta_1,\theta_2) = {} & J_1(2\theta_1)(\theta_2^2/2 - 1) + \theta_2^2[J_1(2\theta_1) - J_3(2\theta_1)]/4 \\
G_5(\theta_1,\theta_2) = {} & 1/2 + J_0(2\theta_1)(3\theta_2^2/8 + \theta_1^2/4 - 1/2) + 3J_2(2\theta_1)/2 \\
& - J_4(2\theta_1)(3\theta_2^2/8 + \theta_1^2/4)
\end{aligned}$$

where $a \equiv 2(K_2 / K_3)(d / \Lambda)^2$ is termed as the "twist ratio" hereafter; $V_{th} = \pi \sqrt{4\pi K_3 / |\Delta\epsilon|}$ is the threshold voltage with $\Delta\epsilon = \epsilon_\perp - \epsilon_{//}$; $I_{th} = (\pi/d)^2(cK_3 / n_0 u)$ is the threshold intensity; $I_r = \sqrt{I_1 I_2} / I_{th}$ and $I_t = I_1 + I_2$; $J_i(2\theta_1)$ is the

Bessel function of first kind of order i. With $\theta_2^2 << 1$, more explicit form of θ_2 can be obtained as

$$\theta_2 \cong \frac{2I_r J_1(2\theta_1)}{1+(K_2/K_3)(2d/\Lambda)^2-[\frac{I_t}{I_{th}}+(\frac{V}{V_{th}})^2][J_0(\theta_1)-J_2(2\theta_1)]-KG_5(\theta_1,0)} \quad (4)$$

The local reorientation angle θ found by numerical method will be illustrated in next section. Here we treat the grating structure as a perturbation on the uniform molecular reorientation induced by the spatially average effective field under the assumptions, $\theta_2^2 << \theta_1^2 << 1$. The analytical solutions are then obtained as

$$\theta_1 = \sqrt{\frac{2b}{1-K}} \quad (5)$$

and

$$\theta_2 = \frac{I_r}{a+b}\sqrt{\frac{2b}{1-K}} \quad (6)$$

where $b \equiv I_t / I_{th} + (V / V_{th})^2 - 1$ is the reduced effective field.

The effective refractive index n(x) for this uniaxial medium averaging over the sample thickness can be expressed as

$$n(x) = \bar{n} + \Delta\bar{n}_{NL}\cos(\frac{2\pi x}{\Lambda}) \quad (7)$$

where $\bar{n} = n_0 + un_0[1-J_0(2\theta_1)] / 4$ is the spatially uniform refractive index and $\Delta\bar{n}_{NL} = un_0\theta_2 J_1(2\theta_1) / 2$ is the modulation index of the grating. For a Kerr medium, the refractive-index change is proportional to the pump intensity, i.e. $\Delta\bar{n}_{NL} = \bar{n}_2\sqrt{I_1 I_2}$. The Kerr coefficient $\bar{n}_2$ becomes

$$\bar{n}_2 \cong \frac{un_0}{I_{th}} \times \frac{b - 2b^2/(1-K)}{(1-K)(a+b)} \quad (8)$$

This coefficient is independent of the spatially modulating pump $2\sqrt{I_1 I_2}\cos(2\pi x/\Lambda)$, although the uniform optical intensity I_t, which acts as a bias rather than the pump here, appears in the expression of the reduced effective field b. It is obvious that the nonlinear coefficient depends not only on the electric bias and material parameters but also on the experimental geometry, such as the sample thickness and the grating period.

The corresponding induced phase shift of the probing beam across the sample is

$$\delta(x) = \delta_0 + \delta_1 \cos(\frac{2\pi x}{\Lambda}) \qquad (9)$$

where $\delta_0 = \bar{n}\,(2\pi/\lambda_0)d$ is the spatial average phase retardation and the modulation amplitude of the phase grating, $\delta_1 = \Delta\bar{n}_{NL}(2\pi/\lambda_0)d$, is approximated as

$$\delta_1 \cong (2\phi d I_r)\ \frac{b - 2b^2/(1-K)}{(1-K)(a+b)} \qquad (10)$$

in the small-reorientation regime with $\phi = \pi u n_0 / \lambda_0$; λ_0 representing the wave length of probing beam. The phase amplitude reaches its maximum δ_{1m} at the reduced effective field of

$$b_{pm} = [a^2 + \frac{(1-K)a}{2}]^{1/2} - a \qquad (11)$$

The diffraction efficiency for the probing beam with intensity I_1, defined as the ratio of the diffraction intensity to the total incident intensity, is derived as

$$\eta = r_1 J_1^2(\delta_1) + r_2 J_2^2(\delta_1) \qquad (12)$$

where $r_1 = I_1 / I_2$, $r_2 = I_2 / I_t$, and $I_1 + I_2 = 1$.

The effect of electric field on the phase grating is exhibited by the factor b in the above equations. The behavior of diffraction efficiency is characterized by the properties of bessel function and the amplitude of the phase modulation. There exists an absolute maximum diffraction efficiency in Eq.(12) with respect to the

unique phase amplitude δ_m which depends on the weights r_1 and r_2 only. We have to look at the problem in two categories [6,7]. Namely, δ_{1m} (the maximum value of δ_1 as a function of b) is greater or less than δ_m.

For $\delta_{1m} \leq \delta_m$ (single peak regime), the diffraction efficiency peaks at one single value of the biased electric field with a maximum of $\eta(\delta_{1m})$. However, when $\delta_{1m} > \delta_m$ (double peak regime), the diffraction efficiency reaches its absolute maximum $\eta(\delta_m)$ at two distinct values of the biased electric field. It can be seen from Eq.(10) that the phase modulation amplitude depends on the period of the phase grating, the three elastic constants and the incident laser intensities. In order word, a double peaks regime can always be obtained by choosing suitable experimental geometry and physical parameters. To illustrate the behavior of the diffraction efficiency with respect to the electric field, the optimal effective fields b_{dm}'s (and so is the optimal bias) are derived for some special cases.

For K = 0,

$$b_{dm}=\begin{cases} \left(\frac{K_2}{K_3}\right)^{1/2}\left(\frac{d}{\Lambda}\right) & \text{, single peak} \\ \dfrac{(2\phi dI_r-\delta_m) \pm [(2\phi dI_r-\delta_m)^2 - 16a\phi dI_r\delta_m]^{1/2}}{8\phi dI_r} & \text{, double peaks} \end{cases} \qquad (13)$$

For a = 0,

$$b_{dm}=\begin{cases} 0 & \text{, single peak} \\ 0 \text{ and } (1-K)\dfrac{2\phi dI_r - (1-K)\delta_m}{4\phi dI_r} & \text{, double peaks} \end{cases} \qquad (14)$$

As long as α is much smaller than one, all the results and equations, excepting Eq.(12), derived for the forward interaction are valid for backward interaction with the total intensity I_t representing the summation of I_1, I_2 and I_3. The diffraction efficiency for the first-order diffraction of reverse incident beam I_3 becomes

$$\eta = \frac{I_4}{I_3} = J_1^2(\delta_1) \tag{15}$$

The unique phase amplitude δ_m corresponding to the maximum of η for the backward geometry is 1.84 and is independent of the weights of pumping intensities.

In order to show the uniqueness of the effect of electric field to the nonlinear wave mixing process, the result is compared with that of the case without biased field but with oblique incident laser beams. For K=0, using the results reported by Fuh *etal* [10] for oblique incident case, we define the angle ratio

$$R_\theta = \frac{\theta_2 \text{ of optimal electric bias}}{\theta_2 \text{ of optimal angle bias}} \tag{16}$$

In the small-reorientation regime, R_θ is approximated to

$$R_\theta \cong \frac{\pi(1+2a)}{4(2a)^{1/2}} \tag{17}$$

This ratio is greater than one for all values of a. It is obvious that the enhancement favors the field-biased case particularly in the regime of small twist ratio a. As the phase amplitude δ_1 is regarded, one can define the phase ratio, R_δ, in the same way as

$$R_\delta \equiv \frac{\delta_1 \text{ of optimal electric bias}}{\delta_1 \text{ of optimal angle bias}} \tag{18}$$

In the small-reorientation regime, R_δ can be approximated as

$$R_\delta \cong 2.42 \frac{(1+2a)(1-\sqrt{2a})}{2+\sqrt{a/2}} \tag{19}$$

where the reduced optical anisotropy u is assumed to be 0.2476. The behavior of R_δ will be shown by numerical calculation in next section.

NUMERICAL RESULTS

In order to illustrate the prominent effect of electric field to DFWM process and the characteristic behavior of this process with respect to the material properties and experimental geometries, numerical calculations have been made from Eqs.(2),(4),(7),(9), and (12). The common parameters used are $n_e = 1.81$, $n_o = 1.57$, $|\Delta\epsilon| = 0.5$ and $I_1 : I_2 = 0.595 : 0.405$. If there is no further declaration, the variable parameters are fixed to be $I_t / I_{th} = 0.0765$, d=100 μm, Λ=100 μm, $K_1 = 5.8 \times 10^{-7}$ dyn, $K_2 = 4 \times 10^{-7}$ dyn and $K_3 = 7.5 \times 10^{-7}$ dyn.

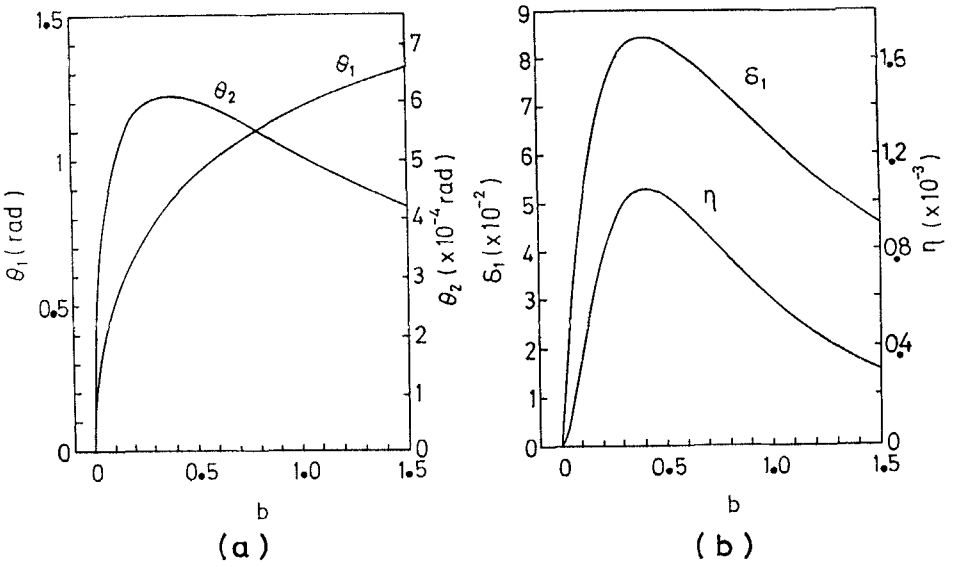

FIGURE 2 General effects of biasing field. Numerical results of (a) reorientation angle θ_1 and θ_2; (b) amplitude of phase grating δ_1 and diffraction efficiency η vs the reduced effective field b with d = 50μm, and $I_t / I_{th} = 0.01$.

The peak shift phenomena are shown by curves of the average reorientational angle θ_1, modulation angle θ_2, phase amplitude δ_1 and diffraction efficiency η versus the reduced effective field b with fixed optical intensity in Fig.2 as predicted by Eq.(6) and (10). In Fig.3, the peak phase amplitude δ_{1m} is increased by increasing the grating period Λ, so that the diffraction efficiency is shifted from single- to double-peak regime.

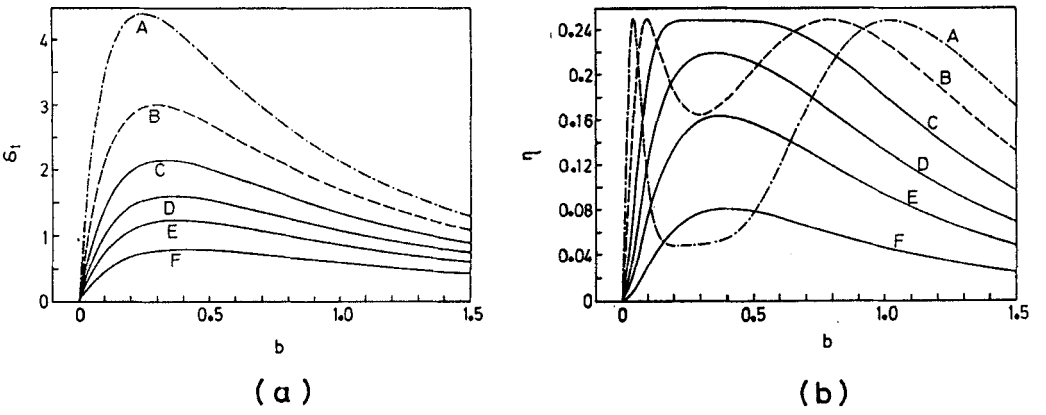

FIGURE 3 Numerical results of (a) phase amplitude δ_1, and (b) diffraction efficiency η vs reduced effective field b. Capitalized letters from A to F represent curves with Λ^{-1} = 0.003, 0.006, 0.01, 0.012, 0.014, and 0.018, respectively.

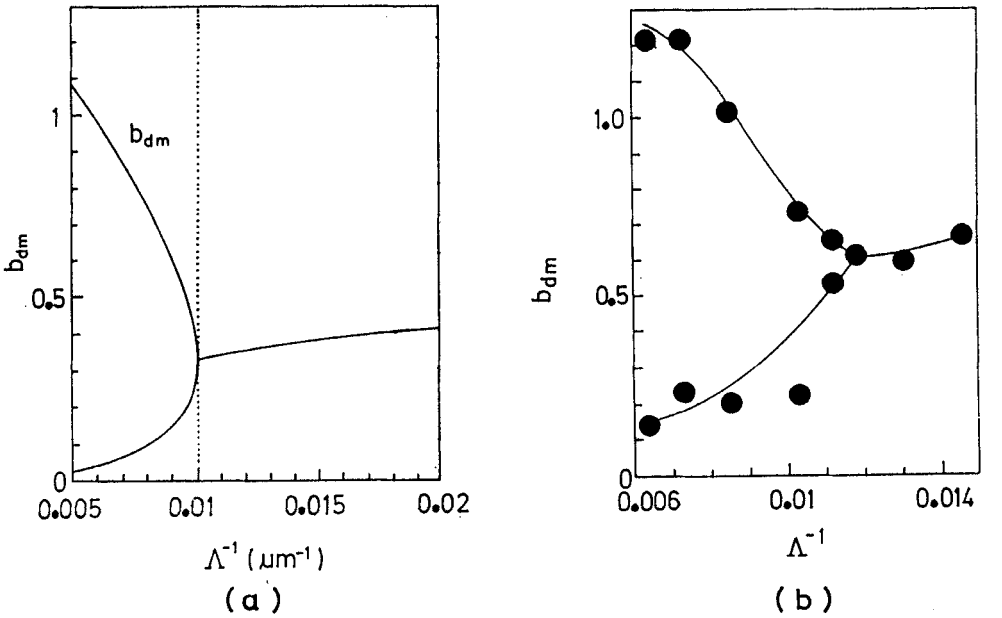

FIGURE 4 Optimal field b_{dm} vs the reciprocal of grating period Λ^{-1}. (a) Numerical results with typical conditions. (b) Experimental results with I_t / I_{th} = 0.209 and d = 110μm.

The optimal bias b_{dm} for diffraction efficiency are found with respect to related variables to exhibit the crucial influence of the twist effect. As shown in Fig.4(a) for small grating period, b_{dm} is a single valued function. However, it becomes a double valued function for sufficient large grating period. This means, for large Λ, that double peaks of diffraction efficiency can be obtained. The peak shift ,e.g., the value of b_{dm}, of first peaks increases as the grating period decreases due to the twist effect.

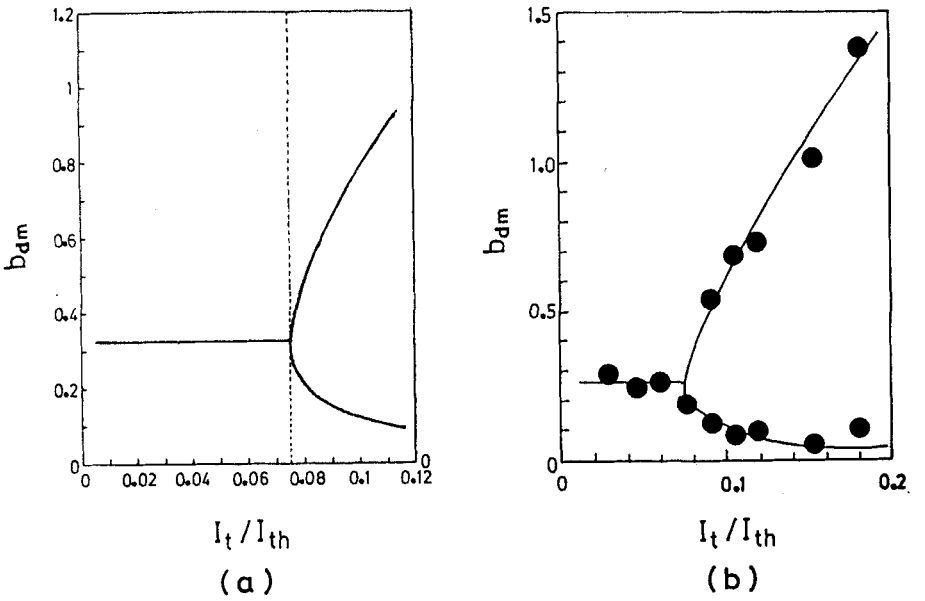

FIGURE 5 Optimal field b_{dm} vs the reduced intensity I_t / I_{th}. (a) Numerical results with typical conditions. (b) Experimental results with d = 92μm and Λ = 146μm. Solid lines are a guide to the eyes.

The effect of the optical intensity is shown in Fig.5(a). It can be understood that a stronger optical pump will induce a more steeply modulated grating then a larger diffraction efficiency can be obtained. It is also seen that b_{dm} is independent of I_t / I_{th} in single peak regime while it spreads out with I_t / I_{th} in the double-peak regime. Therefore, the larger the reduced optical intensity I_t / I_{th} is, the smaller the optimal voltage is needed, since the biasing field b is composed of electric and spatially uniform optical fields.

The physical parameters of NLC materials such as elastic constants will influence the efficiency-optimization problem drastically. Fig.6(a) and 6(b) show the effects of elastic-constant ratios, namely, K_2 / K_3 and $K=1-K_1 / K_3$ which are the intrinsic propaties of the material. The curve in Fig.6(a) exhibits the twist effect by the twist elastic-constant directly. while the behavior of b_{dm} curve in Fig.6(b) is attributed to the competing influences of splay and of bend elastic torques on the molecular reorientation.

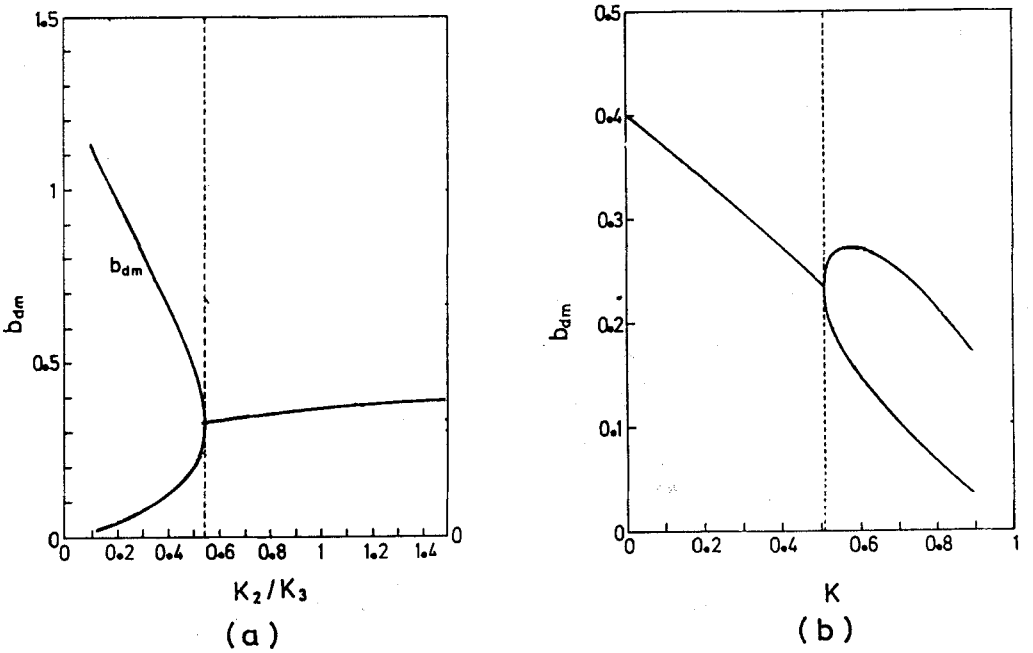

FIGURE 6 Optimal field b_{dm} vs the elastic-constant ratios, (a) K_2 / K_3 and (b) K.

The phase amplitude δ_1 and diffraction efficiency η versus the reduced effective field b for typical condition is shown in Fig.7(a) and 7(b) both for forward and backward interactions. It is obvious that they have similar behaviors.

In order to compare the electric biasing effect with the oblique incident effect, the numerical calculation is made for the reorientational angle θ_2 at the optimal electric bias and optimal angle bias separately. And the angle ratio R_θ, defined in Eq.(16), is plotted versus the twist ratio a as shown in Fig.8(a). The value of R_θ is always greater than one as predicted by the approximated formula in Eq.(17). It is obvious that the enhancement favors the field-biased case, particularly in the regime

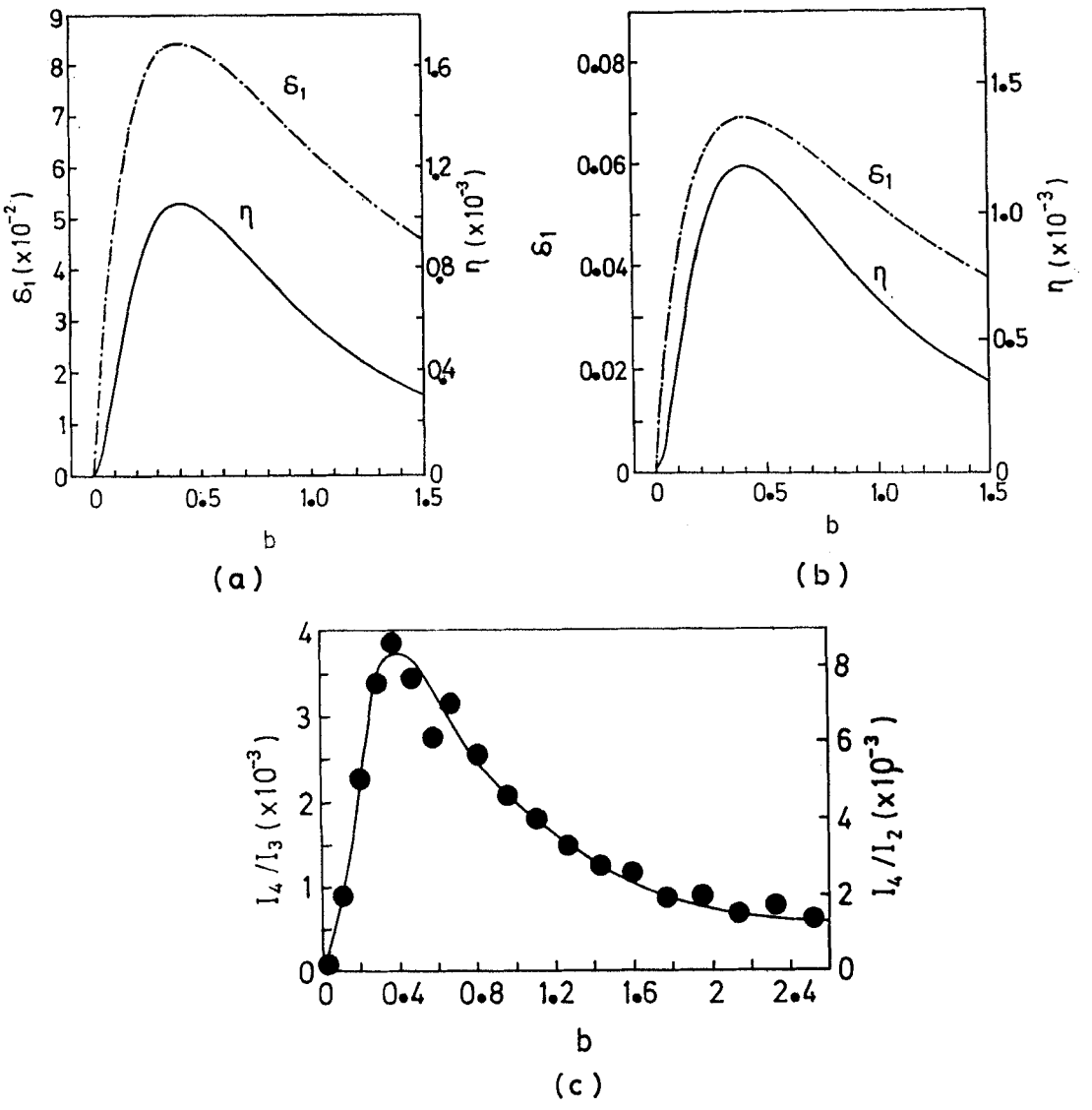

FIGURE 7 Comparison between forward and backward interaction DFWM. Numerical results of phase amplitude δ_1 and diffraction efficiency η versus b for (a) forward interaction (r_1= 0.595 and r_2=0.405), (b) backward interaction (r_1=r_3=0.4 and r_2=0.2). Other parameters are the same as that used in Fig.2. (c) Experimental results of backward interaction with d=75μm, I_t/I_{th} =0.021, and I_1: I_2:I_3=0.71:1:1.6. The solid line is a guide to the eyes.

of small twist ratio, where the optimal biasing field is around the threshold and the critical enhancement of static field on DFWM becomes more significant. Similarly, numerical results of R_δ as calculated according to the definition in Eq.(18), for three different reduced optical anisotropies $u\acute{s}$ are shown in Fig.8(b). In the regime of larger twist ratio, e.g., a=0.5, the optimal phase in normal-incidence case is even smaller than one half of that in oblique-incidence case although the angle ratio R_θ is still larger than one. The fact that an oblique geometry has a longer interaction length for the same sample thickness can account for it. In conclusion, from the application point of view, the normal-incidence geometry with an electric bias can be chosen, especially for a low twist-elastic-constant NLC material.

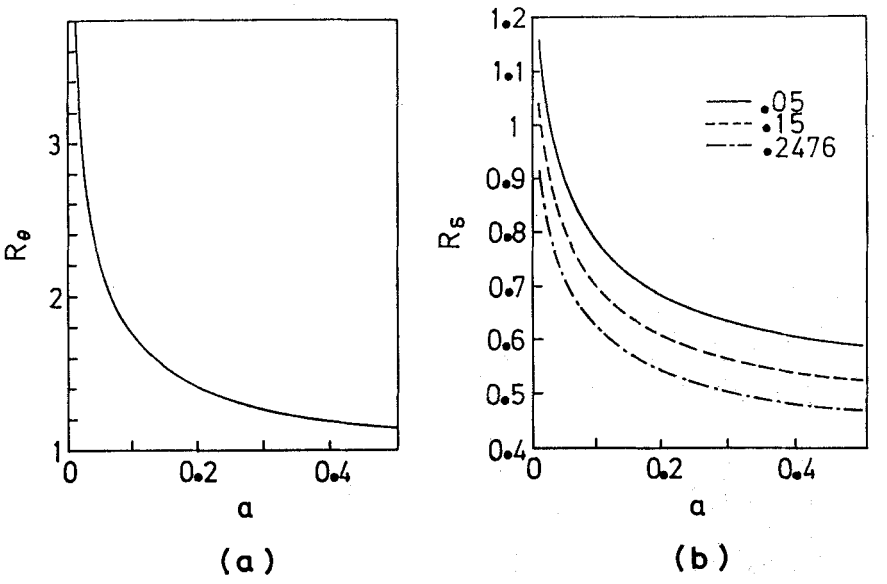

FIGURE 8 Numerical results of (a) optimal reorientation ratio R_θ, and (b) optimal phase-amplitude ratio R_δ versus the twist ratio a with $I_1 : I_2 = 1 : 1$. Other parameters are the same as used in Fig.2.

EXPERIMENTAL RESULTS

The experimental results are obtained for MBBA at 1 KHz biased electric field with Ar^+ laser as light source. The experimental method for forward interaction is the same stated in previous reports[8,9].

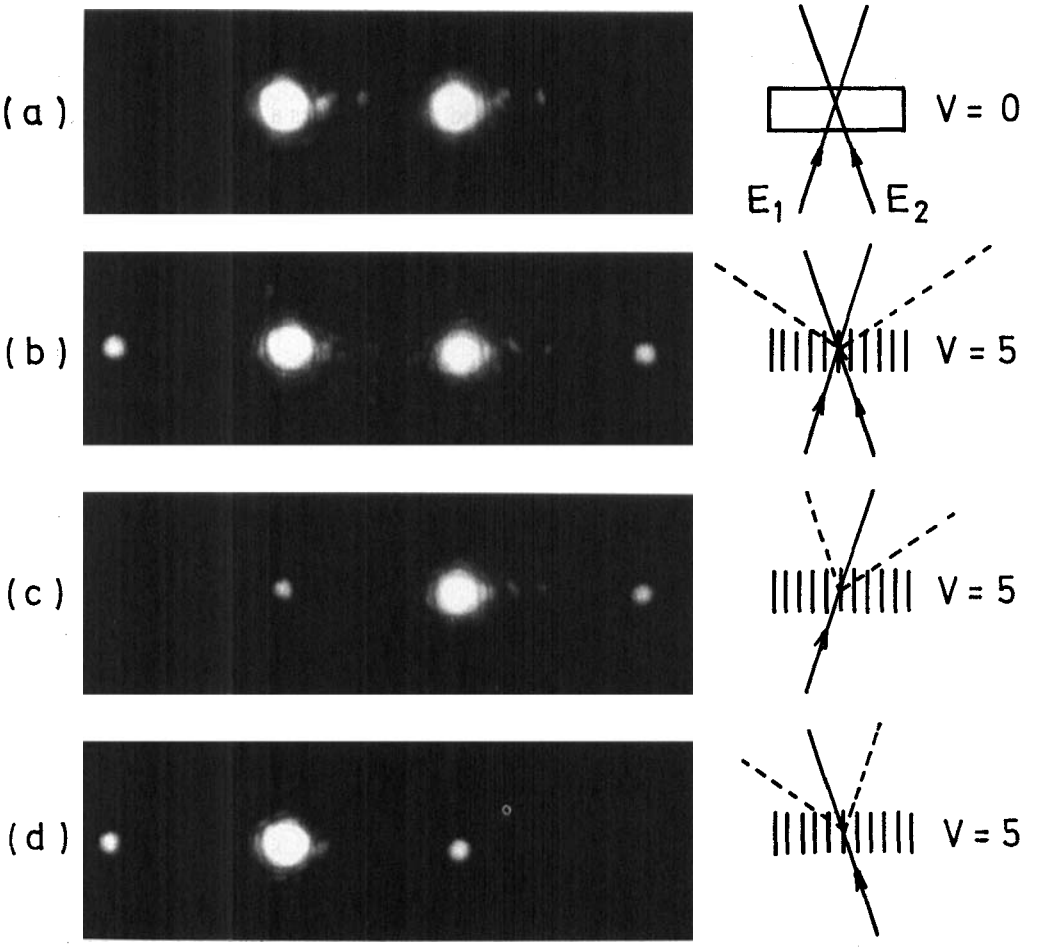

FIGURE 9 Photographs of forward diffraction patterns. Static patterns when both beams on an (a) voltage off, (b) voltage on. Transient patterns when voltage on and (c) beam 2 blocked, (d) beam 1 blocked. Voltage and total intensity are 5 V and 12 W/cm^2, respectively. See Color Plate II.

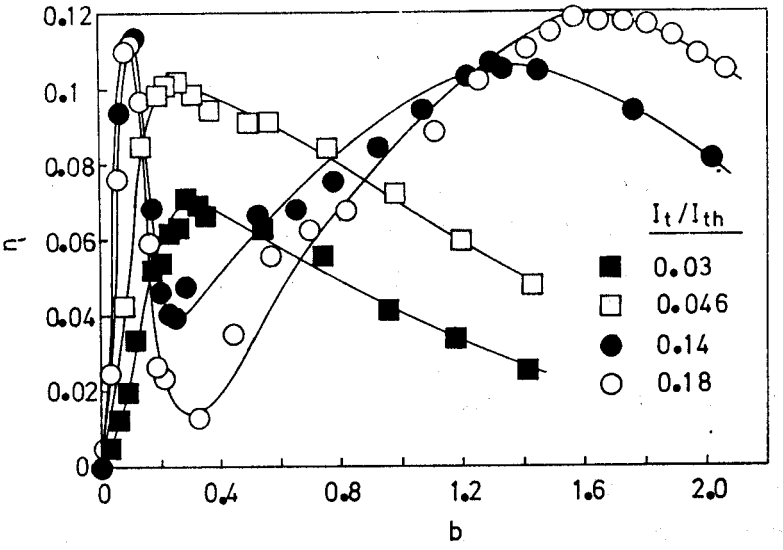

FIGURE 10 Experimental results of the diffraction efficiency versus the reduced effective field for various optical intensities. Solid lines are a guide to the eyes.

We present our observation of optically-induced-grating phenomena at first. The photographs and their corresponding physical pictures are shown in Fig.9. The sample thickness was 75 μm and the grating period was 92 μm. The total incident intensity was about 12.0 W/cm^2. Before the biasing voltage is applied, no significant diffraction spots are observed. This means neither the reorientational nor the thermal grating exists (Fig.9(a)). Two clear diffraction spots with significant scattering noise aside can be seen while a 5-volt bias is applied in the sample (Fig.9(b)). To further check the existence of the phase grating, we took the picture shown in Fig.9(c) sooner after one of the incident beams was blocked. The response time of NLC is fairly slow such that we have sufficient time to take this photograph. This transient pattern is directly derived from the quasi-static phase grating, as schematically depicted aside, which can persist for several seconds. Similar behavior is also shown in Fig.9(d) while the other beam was blocked.

Keeping other parameters fixed, the curves of measured diffraction efficiency versus reduced effective field, for several incident intensities, show both single peak and double peaks with unambiguous peak shifts[7] (Fig.10). The dependence of peak

occurrence[7] on I_t is shown in Fig.5(b). The curve of b_{dm} has the characteristic behavior as the theoretical prediction which is shown in Fig.5(a). The b_{dm} in Fig.4(b) found by experiment spreads out with the increment of Λ as predicted in Fig.4(a)

The backward interaction geometry is shown in Fig.1(c). The intensity of I_4 is measured as the first order diffraction intensity of the reverse incident beam I_3. The result is shown in Fig.7(c). It is in the typical single-peak diffraction regime.

DISCUSSION AND CONCLUSION

The effect of the finite beam size[11] on the threshold intensity can be neglected since the ratio of the spot size to the sample thickness is always larger than 5 in all our experiment. The experimental results exhibit the same behaviors of the curves predicted by the numerical calculation. However, there are some quantitative discrepancies for the following possible reasons. Since a large part of the beam energy is contained in the spurious background scattering, the measured diffraction efficiency is always smaller than what is predicted by the theoretical calculation. In addition, it is difficult to determine the exact optimal bias in the high-optical-field experiments, because the simultaneous occurrence of self-phase modulation[1] effect (several rings are observed in diffraction spot) makes it hard to distinct the diffraction beam from the other spots.

The dependence of the optimal reduced effective field b_{dm} for the diffraction efficiency on the sample thickness is peculier. The detailed calculation and experiment is in progress[9]. Nevertheless, the unique effect of thickness is obvious since the nonlinear refractive index change decreases and the optical path increases as the sample thickness increases. Consequently, the phase amplitude δ_1 peaks at the unique optimal thickness $d_m \cong 0.21\ (K_3 / K_2)^{1/2}\ \Lambda$ instead of increaseing with d monotonically.

In conclusion, the nonlinear DFWM process, including both the forward- and backward-wave interaction geometries, in homeotropically aligned nematic liquid crystals are studied. The prominent effect of electric field to this nonlinear optical process is due to the critical behavior of the sample at the Freedericksz transition.

The third-order nonlinearity of NLCs is characterized by the behavior of the field-induced molecular reorientation and is essentially a Kerr-like effect.

According to the simplified scheme of a thin-sample geometry, a detailed theoretical model including three elastic constants is established to describe he periodically distorted structure of molecular reorientation, the formation of a phase grating and its associated diffraction. The behavior of this DFWM is characterized not only by the intrinsic properties of the NLC material but also by the experimental parameters. The optimal biasing electric field is crucially influenced by the twist deformation in the reorientational grating and the competing influences of splay and of bend elastic torques on the molecules. This is shown by the dependence of optimal reduced effective field, b_{dm} for diffraction efficiency, on the optical intensity I_t, the grating period Λ and the elastic-constant-ratios, namely, K_3 / K_2 and K .

The uniqueness of the electric field effect on the DFWM is shown by comparing the behavior of induce phase grating in field-biased and normal-incidence case with that of the oblique incident geometry without electric bias.

ACKNOWLEDGEMENT

This work was supported by the Chinese National Science Council under contract No. NSC80-0417-M009-02.

REFERENCES

1. S. H. Chen, *etal.*, Opt. Lett., 10, 493 (1985).
2. S. H. Chen and J. J. Wu, Appl. Phys. Lett., 52, 1998 (1988).
3. See, e.g., Y. R. Shen, IEEE J. Quantum Elec, QE-22, 1196 (1986).
4. R. M. Herman and R. J. Serniko, Phys. Rev. A., 19, 1757 (1979).
5. I. C. Khoo, Phys. Rev. A, 25, 1040 (1982).
6. S. H. Chen and C. L. Kuo, Appl. Phys. Lett., 55, 1820 (1989).
7. C. L. Kuo and S. H. Chen, Opt. Lett, 15, 610 (1990).
8. C. L. Kuo and S. H. Chen, J. Appl. Phys., Nov.1 (1990).
9. C. L. Kuo, S. H. Chen, and J. G. Wei, will be published elsewhere.
10. Y. G. Fuh, R. F. Code, and G. X. Xu, J. Appl. Phys. 54, 6368 (1983).
11. I. C. Khoo, T. H. Liu, and P. Y. Yan, J. Opt. Soc. Am. B., 4, 115 (1987).